Journal of Fluorine Chemistry 138 (2012) 34–41

Contents lists available at SciVerse ScienceDirect

Journal of Fluorine Chemistry

journal homepage: www.elsevier.com/locate/fluor

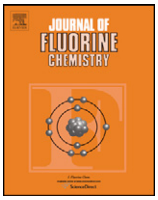

Fluoro-containing poly(amide-imide)s with sterically hindered pendants: Synthesis and characterization

Hossein Behniafar *, Farzin Zardoozi, Ali Rastkar

Chemistry Group, Faculty of Science, Islamic Azad University, Damghan Branch, Damghan, Iran

ARTICLE INFO

Article history:
Received 15 January 2012
Received in revised form 29 February 2012
Accepted 7 March 2012
Available online 16 March 2012

Keywords:
Fluoropolymer
Trifluoromethyl group
Optical behavior
Heat stability
Organo-solubility

ABSTRACT

A structurally kinked fluorinated diacid, 2,6-bis(N-trimellitimido)-4-trifluoromethyl-4′-phenoxydiphenyl ether (TFPDPE) was synthesized and then used for preparing a new class of fluoro-containing poly(amide-imide)s via phosphorylation polyamidation with four diamines including 4,4′-(oxidianiline, 2,6-diamino-4-trifluoromethyl)-4′-phenoxydiphenyl ether, 1,5-bis(2-amino4-trifluoromethylphenoxy)-naphthalene, and 2,2′-bis(2-amino-4-trifluoromethylphenoxy)-1,1′-binaphthyl. Chemical structure of monomer TFPDPE as well as the resulted polymers was fully confirmed by IR and NMR spectroscopy. Limited viscosity numbers ([η]'s) of the resulting polymers at 25 °C were measured. The values of $\bar{M}_w$ and $\bar{M}_n$ were determined using gel-permeation chromatography (GPC). In addition, the absorption edge values (λ_0) obtained from their UV curves were determined, and all the resulting poly(amide-imide)s exhibited high optical transparency. The crystallinity of the polymers was estimated by wide-angle X-ray diffraction (WXRD), and the resulted polymers exhibited nearly an amorphous nature. To study on the surface morphologies, the scanning electron microscopy (SEM) images of the poly(amide-imide)s were taken. Furthermore, solubility of the samples in various kinds of organic solvents was tested. From differential scanning calorimetric (DSC) analyses, the polymers showed T_g's between 304 and 328 °C. Thermo-stability of the polymers was determined by thermogravimetric analysis (TGA), and the 10% weight loss temperatures of the poly(amide-imide)s were found to be in the range of 548–553 °C.

1. Introduction

High-performance polymers such as polyimides, polyamides and poly(amide-imide)s with high glass transition temperature (T_g), high thermal stability, good mechanical properties have been identified for a variety of applications such as engineering plastics of aerospace industries, optical and electronic devices and also as films or membranes [1,2]. However, many completely aromatic polymers do not display ideal properties, resulting from deficiencies in processability and solubility. Insolubility in common organic solvents, intractability, infusibility and strong color often limit their utility in various advanced technological applications. To circumvent the limitations of aromatic polyimides and poly(amide-imide)s some structural modifications often become essential [3–5].

It has been demonstrated that introduction of fluorinated substitutions within the aromatic polyimides and poly(amide-imide)s can give these polymers many desirable properties, making them suitable for a much wider range of applications [6–10]. In this regard, considerable attention has been devoted to the preparation of new classes of fluorine-containing polymers using a large variety of fluorinated monomers [11–15]. The exceptional results corresponding to the synthesis of processable fluoropolymers became more and more in course of time via designing new chemical structures, and it seems that we have to continue this research line for the future. Introduction of –CF_3 group, as the most prominent representative among perfluoro alkyl groups, into aromatic structure of a high-performance polymer has been one of the most widely used strategies to enhance processability along with a desired set of properties for the resultant polymer [16–21]. This introduction modifies several physical properties, e.g., increases solubility, thermal stability, optical transparency and flame-resistance, while simultaneously decreasing the crystallinity, dielectric constant, water absorption, and color intensity. Moreover, owing to the presence of –CF_3 substituents, the formation of charge-transfer complex, which imparts deep yellow color to the polymer, is largely hindered, and thus the color intensity is considerably reduced, making the polyimide more suitable for some applications. On the other hand, polymers with structurally hindered chains caused by local steric crowding along the chains indicate improved processability relative to those of lacking steric hindrance because of a constrained macromolecular twisting [22–24,7]. These structural congestions can be generally resulted from the presence of

---

* Corresponding author.
E-mail address: h_behniafar@du.ac.ir (H. Behniafar).

0022-1139/$ – see front matter © 2012 Elsevier B.V. All rights reserved.
doi:10.1016/j.jfluchem.2012.03.009

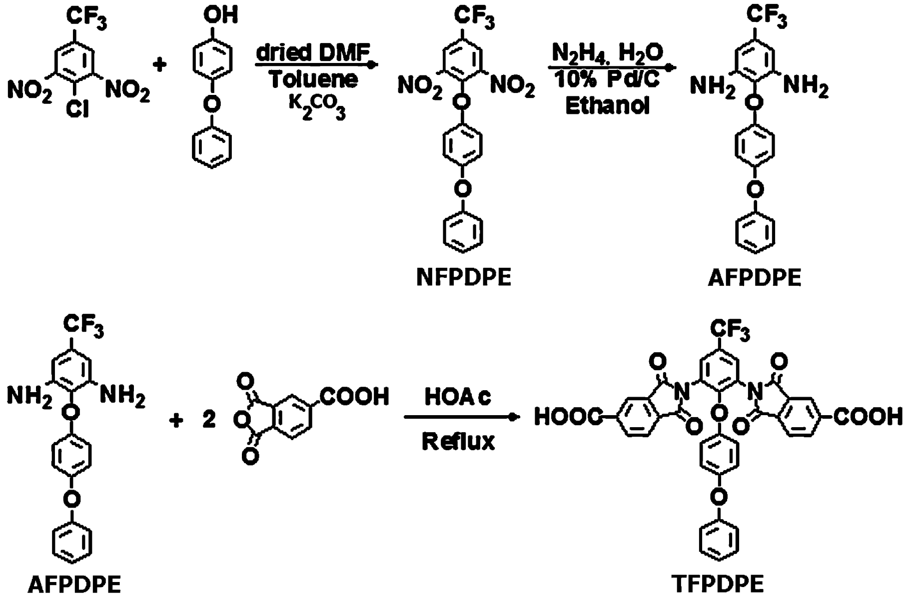

Scheme 1. Synthesis of fluoro-containing monomer TFPDPE.

voluminous substituents in close places into a macromolecular chain such as *ortho* positions of an aromatic ring.

Therefore, alongside our recent studies [25–30], this research focuses on the synthesis of a structurally hindered imide-containing fluoro-diacid, 2,6-bis(N-trimellitimido)-4-trifluoromethyl-4′-phenoxydiphenyl ether (TFPDPE) via a three-step reaction. The diacid TFPDPE has been designed as a potentially suitable monomer for poly(amide-imide)s, capable of imparting good processability and high thermal stability at the same time. The poly(amide-imide)s obtained from TFPDPE were characterized by IR, NMR, solution viscometry, GPC, UV–vis, WXRD, organo-solubility, SEM, DSC and TGA.

2. Results and discussion

2.1. Dinitro and diamine precursors

Scheme 1 (upside) shows the synthetic route to 2,6-diamino-4-trifluoromethyl-4′-phenoxydiphenyl ether (AFPDPE) by a two-step process. In the first step, aromatic nucleophilic displacement of 4-chloro-3,5-dinitrobenzotrifluoride with 4-phenoxyphenol in the presence of anhydrous K_2CO_3 in DMF solvent resulted in 2,6-dinitro-4-trifluoromethyl-4′-phenoxydiphenyl ether (NFPDPE) as a pale yellow solid. In the second step, this dinitro was reduced in ethanol in the presence of hydrazine hydrate and a catalytic amount of palladium on activated carbon at 80 °C to produce white crystals of the fluorinated diamine AFPDPE. The structures of dinitro NFPDPE and diamine AFPDPE were confirmed by IR and NMR spectroscopic methods. In the IR spectrum of dinitro NFPDPE the peaks attributed to the stretching vibrations of the bonds Ar–O and C–F appeared at 1267, 1183, 1141, and 1101 cm^{-1}. Moreover, absorptions appearing around 1322 and 1545 cm^{-1} are due to symmetric and asymmetric stretching of $-NO_2$ groups, respectively. In the ^1H NMR spectrum of NFPDPE two hydrogens attached to the nitro-containing ring (Ha) resulted in a singlet centralized at 8.42 ppm. Furthermore, in the ^{13}C NMR spectrum, twelve peaks corresponding to the twelve kinds of aromatic carbons appeared in the range of 120.3–150.8 ppm. In this spectrum, the quartets of the heteronuclear $^{13}C–^{19}F$ coupling appear in the region of 121.2–128.1 ppm. The coupling constant of one-bond C–F is about 280 Hz and two-bond is about 35 Hz, respectively. Thereby all these spectral patterns are thoroughly in agreement with the proposed structure of dinitro NFPDPE. In the IR spectrum of diamine AFPDPE the characteristic absorption of nitro groups disappeared and the characteristic bonds of amino groups at 3460 and 3375 cm^{-1} (N–H stretching) and 781 cm^{-1} (N–H out of plane bending) appeared after reduction. In the ^1H NMR spectrum of diamine AFPDPE the signals of aromatic protons appear in the range of 6.75–7.64 ppm, and the characteristic resonance signal at 4.97 ppm is due to the amino group. In the ^{13}C NMR spectrum of diamine AFPDPE the twelve aromatic carbons appeared their signals in the range of 110.7–152.2 ppm. Moreover, the quartets of the heteronuclear $^{13}C–^{19}F$ coupling appear in the region of 121.4–128.1 ppm. The coupling constant of one-bond C–F is about 260 Hz and two-bond is about 35 Hz, respectively.

2.2. Fluorinated diimide–diacid TFPDPE

Scheme 1 (underside) shows the reaction to CF_3-containing diimide–diacid TFPDPE. In this reaction, ring-opening addition of diamine AFPDPE to trimellitic anhydride in refluxing glacial acetic acid results in the corresponding di(amic–acid) intermediate. Next, an intramolecular cyclodehydration can give rise to the related cyclic imide groups. The FT-IR spectrum of monomer TFPDPE showed the characteristic absorption bands around 2400–3600 cm^{-1} (–OH, carboxylic acid), 1783 cm^{-1} (imide C=O asymmetrical stretching), and 1723 cm^{-1} (imide C=O symmetrical stretching and acid C=O stretching), confirming the presence of imide ring and carboxylic acid groups in the structure. The ^1H NMR spectrum of TFPDPE presented three specified signals around the downfield regions (8.14–8.50 ppm) due to the trimellitic acid moiety. Moreover, the protons for the carboxylic acid groups are observed at about 13.60 ppm in the form of a short and broad peak. The ^{13}C NMR spectrum of TFPDPE exhibited eighteen peaks of various absorptions for aromatic carbons. In this spectrum, carbons of carboxylic acid and imide groups were observed at about 164.0 ppm. Fig. 1 displays IR (top), ^1H NMR (middle), and ^{13}C NMR (bottom) spectra of the synthesized monomer.

2.3. Preparation of fluorinated poly(amide-imide)s

According to the phosphorylation technique first described by Yamazaki and Higashi [31] a series of novel poly(amide-imide)s were synthesized from diacid TFPDPE and various diamines as

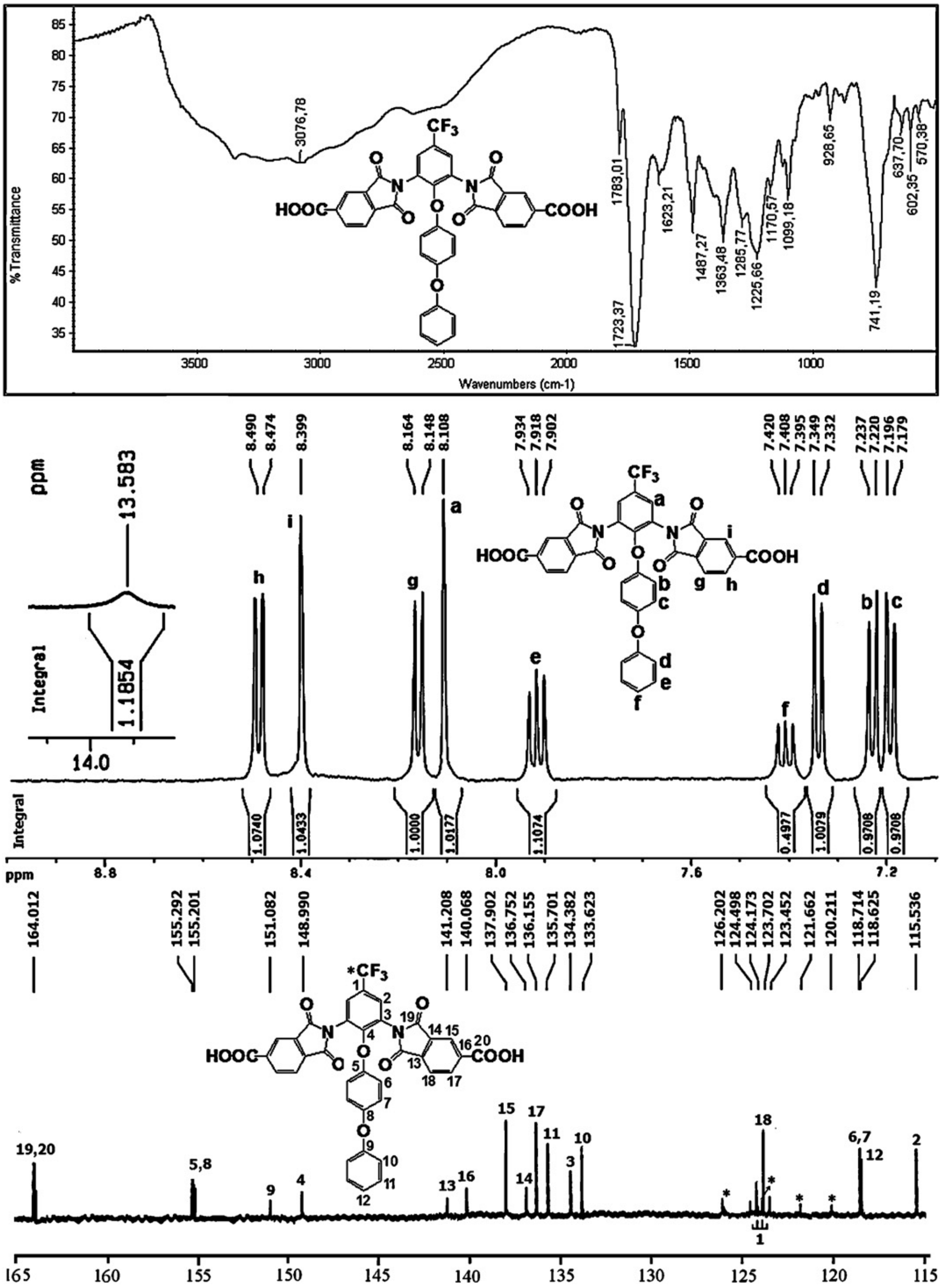

Fig. 1. IR (top), ^{1}H NMR (middle), and ^{13}C NMR (bottom) spectra of monomer TFPDPE.

shown in Scheme 2. It should be noted that the selection of the diamine comonomers was well-advised as well. Three of them possess CF_3 group in their chemical structures. This in turn can help the preparation of low-colored, optically transparent and organo-soluble polymers when combining to diacid TFPDPE. In the case of AFPBN, in addition to the presence of two trifluoromethyl groups and two ether linkages in its structure, it profits greatly from a twisting about the bond linking the two naphthyl rings. All the polycondensations were homogeneously throughout the reactions and afforded highly viscous polymer solutions with up to 90% yield. Limited viscosity numbers ($[\eta]$'s) of the resulting poly(amide-imide)s in DMAc at 30 °C as well as the results of GPC analyses are tabulated in Table 1. The obtained polymers had limited viscosity numbers in the range of 0.62–0.75 dL g^{-1}. These values for all polymeric solutions were determined through the extrapolation of the concentrations used to zero. Furthermore, the poly(amide-imide)s had polydispersity index (PDI) values of about two. The molecular weights of these polymers were high enough to obtain flexible and tough thin films by casting from their appropriate solutions.

The formation of the products was confirmed by FT-IR and NMR spectroscopy methods. The FT-IR spectra of the CF_3-containing poly(amide-imide)s exhibited the characteristic amide bands at about 3400 (N–H stretching) and 1650 (C=O stretching) cm^{-1}. The resulting polymers also showed characteristic imide bands around 1780 and 1720 cm^{-1} (asymmetrical and symmetrical C=O

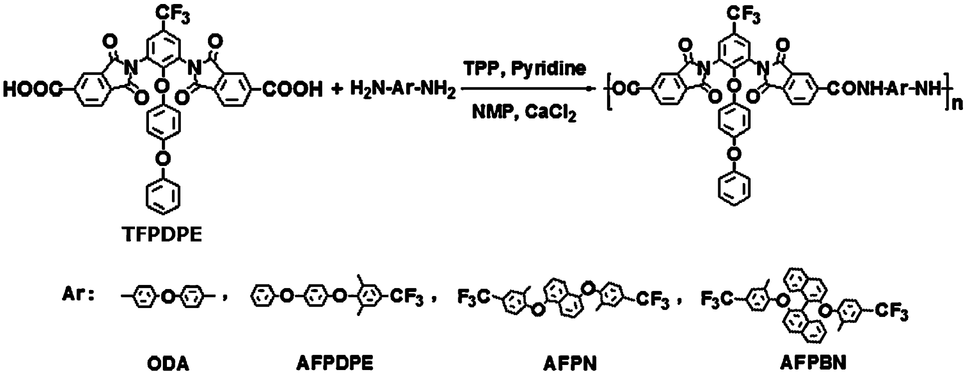

Scheme 2. Preparation of fluorinated poly(amide-amide)s.

Table 1
Some characteristics of the resulting poly(amide-imide)s.

Polymer	$[\eta]$[a] (dL g^{-1})	$\bar{M}_w$[b] (g mol^{-1})	$\bar{M}_n$[b] (g mol^{-1})	PDI[c]	λ_0[d] (nm)
TFPDPE/ODA	0.68	18,800	9300	2.02	379
TFPDPE/AFPDPE	0.62	21,400	11,500	1.86	374
TFPDPE/AFPN	0.75	26,900	12,500	2.15	375
TFPDPE/AFPBN	0.71	32,100	13,600	2.36	378

[a] Measured in DMAc at 25 °C.
[b] Measured by GPC in THF with polystyrene as a standard.
[c] Polydispersity index.
[d] Cut-off wavelength is defined as the point at which the light transmittance from the prepared thin films becomes less than 1%.

stretching vibrations, respectively) and 1380 (imide C–N stretching). In these spectra, lacking the highly broad absorption peak in the region 2400–3500 cm^{-1}, related to acid O–H stretching, indicates that no any TFPDPE monomer is present in the sample composition. Instead, in the left side of this region a peak corresponding to N–H stretching appeared at about 3400 cm^{-1} as stated. In the ^{1}H NMR spectra of the resulting poly(amide-imide)s, the existing aromatic protons resonate in the region 7.1–8.5 ppm. Among the aromatic protons, the protons adjacent to the imide ring appeared at the farthest downfield. In addition, the signals appeared at the most downfield region, about 10.50 ppm, could be attributed to the protons of the amide linkages. Fig. 2 shows representative IR (top) and ^{1}H NMR (bottom) spectra of the poly(amide-imide)s TFPDPE/AFPDPE and TFPDPE/ODA, respectively.

2.4. Optical behavior

To investigate the optical behavior of the resulting fluoropoly(amide-imide)s, their solutions (10^{-5} mol L^{-1} in DMSO) were separately prepared, and then exposed to UV–vis rays. Over 80% of irradiated light could be transmitted from all the solutions in the wavelength range of 500–750 nm. Furthermore, the absorption edge values (λ_0's) are determined at below 380 nm. These observations obviously show that the resultant fluoro-containing macromolecules have high level of optical transparency in the UV–vis light region. As mentioned earlier, the formation of charge-transfer complex is largely prevented with –CF$_3$ substituents, and thereby the absorption intensity is remarkably lowered. The spectra of the solutions were nearly identical with each other. Table 1 (the last column) lists the values of λ_0 obtained from the diluted solutions of the polymers in DMSO.

2.5. WXRD studies

The crystallinity of the resulting poly(amide-imide)s was measured by wide-angle X-ray diffraction (WXRD) at room temperature with 2θ ranging from 5° to 40°. The resulted diffractograms clearly showed that the mentioned poly(amide-imide)s were essentially amorphous, and no remarkable crystal diffraction appeared in their WXRD curves. Apparently, the laterally attached –O–Ph–O–Ph bulky group, which itself has been

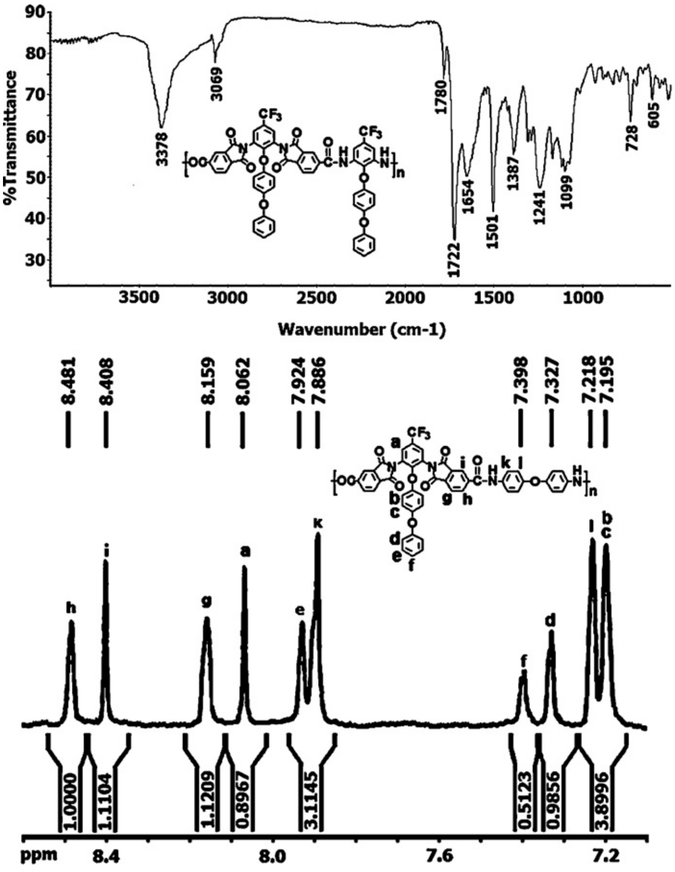

Fig. 2. IR spectrum of polymer TFPDPE/AFPDPE (top), and ^{1}H NMR spectrum of polymer TFPDPE/ODA (bottom).

Table 2
Solubility of the resulting fluorinated poly(amide-imide)s.

Polymer	DMSO	DMF	DMAc	NMP	Pyridine	THF	Toluene
TFPDPE/ODA	++	++	++	++	+	–	–
TFPDPE/AFPDPE	++	++	++	++	++	±	±
TFPDPE/AFPN	++	++	++	++	++	±	–
TFPDPE/AFPBN	++	++	++	++	++	±	±

Qualitative solubility: 10 mg. mL^{-1}.
DMSO, dimethylsulfoxide; DMF, N,N-dimethylformamide; DMAc, N,N-dimethylacetamide; NMP, N-methyl-2-pyrrolidinone; THF, tetrahydrofuran.
++, soluble at room temperature; +, soluble on heating; ±, partially soluble; –, insoluble.

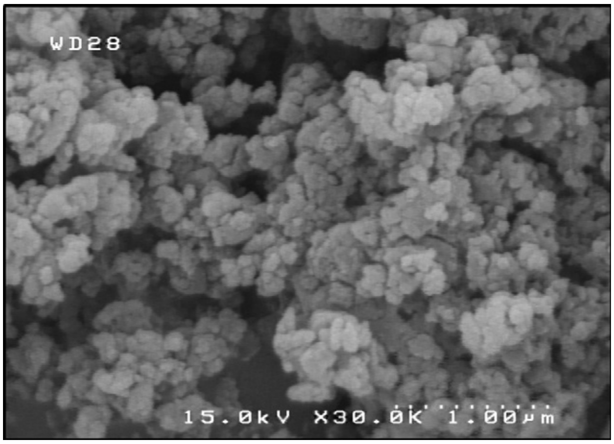

Fig. 3. SEM image of poly(amide-imide)s TFPDPE/AFPDPE.

sandwiched between two *ortho* trimellitimido groups decreases the chain–chain interactions, resulting in a decreasing crystallinity. In fact, this structural crowding provides the chains a non-coplanarity, leading to disordered kinked macromolecules. Moreover, the effect of the diamine comonomers on the crystallinity amount could be observed by comparing the unequal shape of the diffractograms obtained. By comparing the diffractograms obtained, it is concluded that the amorphousness nature of poly(amide-imide)s TFPDPE/ODA is somewhat lower than that of the other ones. This might be attributed to the lesser macromolecular prevention of diamine moiety against compactness in this polymer.

2.6. Organo-solubility

The solubility behavior of the resulting poly(amide-imide)s was tested qualitatively in various organic solvents, and the results were tabulated in Table 2. All the polymers were readily soluble in high polar solvents such as DMSO, DMF, DMAc, and NMP at room temperature. Except poly(amide-imide)s TFPDPE/ODA the remainder ones were dissolved even in pyridine as a moderate polar solvent at room temperature. These structurally well-designed polymers were even partially soluble in THF upon heating at about 70 °C. A steric overcrowding caused by the presence of –CF_3 and –O–Ph–O–Ph voluminous groups could be resulted in local non-coplanarities along the chains, and consequently excellent solubility could be observed in tested organic solvents. Moreover, the presence of additional CF_3 polar groups in poly(amide-amide)s TFPDPE/AFPDPE, TFPDPE/AFPN and TFPDPE/AFPBN plays an important role in solubility enhancement of these polymers. The high organo-solubility of poly(amide-imide)s TFPDPE/AFPBN might be also attributed the participation of the two twisted binaphthyl rings, which provides more distortion of the chains. In fact, the excellent organo-solubility of these polymers could be interpreted based on a combination of steric and electronic effects. The bulky arylene-ether pendant groups attached to the CF_3-containing backbone can inhibit the close packing of the macromolecular chains and endow a large amount of polarity due to the high electronegativity of fluorine atoms, and thereby these fluoropoly(amide-imide)s show good organo-solubility, particularly in polar solvents.

2.7. Surface morphology

A representative scanning electron microscopy (SEM) image of poly(amide-imide)s TFPDPE/AFPDPE is shown in Fig. 3. As can be seen, this image clearly shows an agglomerated spherical bulk with non-equal packing, indicating a nearly non-uniformity in the surface area of the samples. The SEM images of the other poly(amide-imide)s showed even more disordered pattern, and no specified shape could be detected for the arrangement of the microstructures obtained. This kind of surface morphology might be attributed to the same amorphous structures, which could be supported by WXRD analyses. Steric factors associated with the previously mentioned bulky substituents could greatly destroy the regularity of the macromolecular main chains and caused a high degree of non-uniformity in microstructural order.

2.8. DSC measurements

Differential scanning calorimetry (DSC) was used to determine the glass-transition temperature values (T_g's) of the samples obtained with a heating rate of 10 °C min^{-1} under nitrogen. Fig. 4(top) shows a typical DSC thermogram of poly(amide-imide)s TFPDPE/AFPDPE. The T_g values were read at the middle of the first break down observed in the DSC plots, and found to be in the range of 304–328 °C. In general, molecular packing and chain rigidity are among the main factors influencing on T_g values. In polymer TFPDPE/AFPDPE the increased rotational barrier resulted from the additional –CF_3 and phenoxy substituents enhanced the T_g value

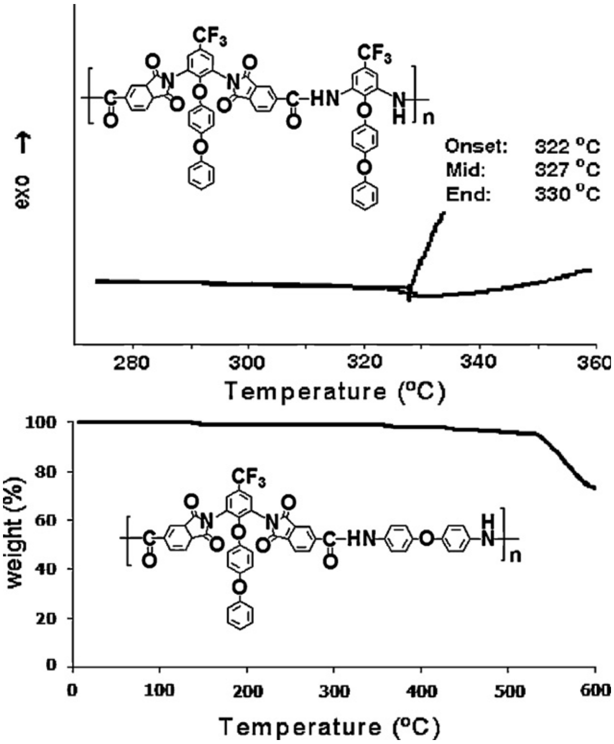

Fig. 4. DSC plot of TFPDPE/AFPDPE (top) and TGA thermogram of TFPDPE/ODA (bottom).

Table 3
Thermal behavior of the resulting poly(amide-imide)s.

Polymer	T_0 [a] (°C)	T_g [b] (°C)	$T_{d5\%}$ [c] (°C)	$T_{d10\%}$ [d] (°C)	CY[e] (wt.%)
TFPDPE/ODA	301	304	532	548	73
TFPDPE/AFPDPE	323	327	538	551	74
TFPDPE/AFPN	312	316	540	553	68
TFPDPE/AFPBN	321	328	533	549	66

[a] Onset temperature, from DSC measurements in N_2, defines the point at which the first deviation from the base line on the low temperature side is observed.
[b] Glass-transition temperatures from the DSC traces in N_2 at heating rate of 10 °C min^{-1}.
[c] Temperature of 5% weight loss, determined by TGA in N_2 at a heating rate of 10 °C min^{-1}.
[d] Temperature of 10% weight loss, determined by TGA in N_2 at a heating rate of 10 °C min^{-1}.
[e] Char yield: residual weight percentages at 600 °C, determined by TGA in N_2 at a heating rate of 10 °C min^{-1}.

relative to the T_g value of polymer TFPDPE/ODA up to 23 °C. A further rotational barrier, and consequently higher T_g value could be also observed by incorporation of rigid and kinked binaphthyl units in polymer TFPDPE/AFPBN chains. Therefore, in addition to diacid TFPDPE, the values of T_g were affected by diamine moieties too, which shows the order AFPBN > AFPDPE > AFPN > ODA as illustrated in Table 3.

2.9. Thermo-stability

The thermo-stability of the resulting fluorinated poly(amide-imide)s were evaluated by thermogravimetric analysis (TGA) under nitrogen atmosphere at a heating rate of 10 °C min^{-1}, and corresponding weight loss temperatures of 5% and 10% ($T_{5\%}$ and $T_{10\%}$) were all determined from original TGA curves. All the aromatic poly(amide-imide)s exhibited good thermal stability with insignificant weight loss up to 550 °C in nitrogen. The $T_{5\%}$ and $T_{10\%}$ values of the poly(amide-imide)s were measured in the ranges of 532–540 and 548–553 °C, respectively. The amount of carbonized residue (char yield) of these fluorinated polymers in nitrogen atmosphere was up to 70% at 600 °C. The high char yields of these polymers could be ascribed to their chemical structure, which has high degree of aromaticity. Obviously, the data from thermal analysis showed that these poly(amide-imide)s have fairly high thermal stability in comparison with many of their analogs. Furthermore, the diamine comonomers have no considerable effect on the heat stabilities. Meanwhile, by comparing the data of poly(amide-imide)s TFPDPE/ODA and TFPDPE/AFPDPE it is proved that no undesired effect on the heat stability of the product could be observed by the introduction of fluoro-containing substituent into the structures. Typical TGA curves of representative poly(amide-imide)s TFPDPE/ODA is shown in Fig. 4 (bottom). In addition, the results obtained from these analyses are completely tabulated in Table 3.

3. Conclusions

A fluoro-containing diimide–diacid (TFPDPE) with high degree of crowding in its chemical structure was successfully synthesized and used to prepare a novel class of aromatic fluorinated poly(amide-imide)s with kinked macromolecules. The incorporation of CF_3 polar substituents as well as arylene-ether voluminous groups, which are sandwiched between two *ortho*-catenated trimellitimido groups could distort the macromolecular chains, and consequently increase their organo-solubility. On the other hand, this new design could also endow a high degree of optical transparency in the prepared solution of the products. In addition, thermal stability of the resulting polymers was not lowered by this structural modification. In summary, these fluoro-containing poly(amide-imide)s displayed excellent organo-solubility, low crystallinity, reasonable thermal stability and glass transition temperatures, making them suitable for thermo-forming processing.

4. Experimental

4.1. Materials

Trimellitic anhydride (TMA) and triphenyl phosphite (TPP) were purchased from Aldrich Chemical Co. and used as received without further purification. All other chemicals were purchased from Merck Chemical Co. 4-Phenoxyphenol and 4-chloro-3,5-dinitrobenzotrifluoride were used as received. 4,4′-Oxydianiline (ODA) was purified by recrystallization from ethanol before use. Diamine AFPDPE was synthesized during the synthesis reaction of the monomer TFPDPE. 1,5-Bis(2-amino4-trifluoromethylphenoxy)naphthalene (AFPN) and 2,2′-bis(2-amino-4-trifluoromethylphenoxy)-1,1′-binaphthyl (AFPBN) were synthesized and purified by procedures reported elsewhere [29,32]. Reagent-grade calcium chloride was dried under vacuum at 180 °C before use. N,N-dimethylacetamide (DMAc), N,N-dimethylformamide (DMF), dimethylsulfoxide (DMSO), N-methyl-2-pyrrolidone (NMP), and pyridine were purified by distillation under reduced pressure over calcium hydride and stored over 4-Å molecular sieves. Hydrazine monohydrate and 10% palladium on activated carbon were used as received. Tetrahydrofuran (THF) and toluene were dried by sodium before use.

4.2. Measurements

Melting points were determined in open capillaries with IA 9200 Series Digital Melting Point apparatus. FT-IR spectra were recorded on a PERKIN ELMER RX I FT-IR spectrometer. The spectra of solids were obtained using KBr pellets. ^1H NMR spectra were recorded with a Bruker AVANCE 500 NMR operated at 500 MHz in dimethylsulfoxide-d_6 (DMSO-d_6) using tetramethylsilane as an internal standard. ^{13}C NMR spectra were also taken with the same apparatus operated at 125 MHz. Viscosity numbers (η_{red}) were measured using an Ubbelohde viscometer with polymer solutions in DMAc at 30 °C. These values were separately measured for concentrations 0.10, 0.25, and 0.50 g dL^{-1}, and then plotted against these concentrations. To determine limited viscosity numbers ([η]) a linear extrapolation was finally done to zero concentration as the *y*-axis intersect [33]. Weight- and number-average molecular weights of the resulting poly(amide-imide)s were determined by gel-permeation chromatography (GPC). This chromatography was performed on a Waters 150-C instrument using Styragel columns and a differential refractometer detector. The molecular weight calibration was carried out using polystyrene standards. Calibration and measurements were made at a flow rate of 1 mL min^{-1} with tetrahydrofuran (THF) as the eluent. Cut-off wavelength (absorption edge) values (λ_0) of the prepared solutions in DMSO at a concentration of 10^{-5} mol L^{-1} were determined with a PERKIN ELMER PTP-1 Peltier System Lambda 25 UV/VIS Spectrometer. Wide-angle X-ray diffraction patterns were performed at room temperatures with film specimens on a Bruker Advance D5 X-ray diffractometer with Ni-filtered Cu/Ka radiation (30 kV, 25 mA). The morphologies of the samples were determined with a HITACHI S-4160 scanning electron microscope (SEM). Thermal gravimetric analysis (TGA) and differential scanning calorimetry (DSC) were performed on a Mettler TA 5000 system (Columbus, OH) under nitrogen atmosphere at a heating rate of 10 °C min^{-1}.

4.3. Synthesis of 2,6-dinitro-4-trifluoromethyl-4′-phenoxydiphenyl ether (NFPDPE)

In a three-necked round bottom flask equipped with a nitrogen inlet, 4-phenoxyphenol (1.8621 g, 10 mmol) and anhydrous potassium carbonate (2.902 g, 21 mmol) were suspended in a mixture of dry DMF (10 mL) and toluene (4 mL). The mixture was then refluxed at 140 °C using a Dean-Stark trap to remove small amount of water azeotropically. After most of the toluene was distilled, 4-chloro-3,5-dinitrobenzotrifluoride (2.7055 g, 10 mmol) was added when the mixture was cooled to 60 °C. The mixture was then allowed to warm to 120 °C and kept for 6 h. After cooling to 25 °C, it was poured into 50 mL of CH_3OH/H_2O to give a yellow solid. After filtration under reduced pressure, the crude product was washed twice with hot water. After drying, the product was recrystallized from DMF/H_2O to give 3.1102 g of NFPDPE as a pale yellow fine crystals (74% yield, m.p. = 83–85 °C).

FT-IR (KBr; cm^{-1}): 1545, 1322 ($-NO_2$ stretch), 1267, 1183, 1141, 1101 (C–F and C–O stretch). ^{1}H NMR (DMSO-d_6; δ, ppm): 8.42 (s, 2H, Ha), 7.87 (t, J = 9 Hz, 2H, He), 7.30 (t, J = 9 Hz, 1H, Hf), 7.22 (d, J = 7 Hz, 2H, Hb), 7.05 (d, J = 9 Hz, 2H, Hd), 6.91 (d, J = 7 Hz, 2H, Hc). ^{13}C NMR (DMSO-d_6; δ, ppm): 150.78 (C9), 144.89 (C4), 143.25 (C5), 143.18 (C8), 141.91 (C3), 133.10 (C11), 131.22 (C2), 128.12 (C*), 125.73 (C*), 124.58 (C12), 123.53 (C*), 122.30 (C1, quartet, $^2J_{C-F}$ = 35 Hz), 121.24 (C*), 120.71 (C10), 120.40 (C6), 120.35 (C7).

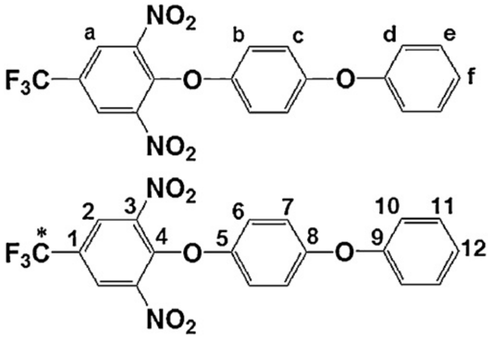

4.4. Synthesis of 2,6-diamino-4-trifluoromethyl-4′-phenoxydiphenyl ether (AFPDPE)

To a suspension of the purified dinitro compound (NFPDPE) (4.2030 g, 10 mmol) and 10% Pd/C (0.02 g) in ethanol (15 mL), hydrazine monohydrate (1.5 mL) was added dropwise to the stirred mixture at 70 °C within 10 min. After complete addition, the mixture was heated at the reflux temperature for another 2 h. The reaction solution was filtered hot to remove Pd/C, and the filtrate was then filtered cold to remove the solvent. The crude product was purified by recrystallization from ethanol to give 2.7385 g of AFPDPE as a pale-cream needles (76% yield, m.p. = 109–113 °C).

FT-IR (KBr; cm^{-1}): 3460, 3375 (N–H stretch), 1618, 1590 (C=C aromatic), 1223, 1199, 1163, 1116 (C–F and C–O stretch), 781 (N–H out of plane bending). ^{1}H NMR (DMSO-d_6; δ, ppm): 7.64 (t, J = 6 Hz, 2H, He), 7.15 (t, J = 6 Hz, 1H, Hf), 7.09 (d, J = 9 Hz, 2H, Hb), 7.01 (d, J = 6 Hz, 2H, Hd), 6.93 (d, J = 9 Hz, 2H, Hc), 6.75 (s, 2H, Ha), 4.97 (s, 4H, Hg). ^{13}C NMR (DMSO-d_6; δ, ppm): 152.20 (C9), 149.18 (C5), 149.01 (C8), 142.65 (C4), 141.01 (C3), 130.64 (C11), 128.10 (C*), 125.73 (C1, quartet, $^2J_{C-F}$ = 35 Hz), 125.48 (C*), 123.25 (C*), 122.52 (C12), 121.44 (C*), 116.50 (C10), 115.88 (C6), 115.85 (C7), 110.68 (C2).

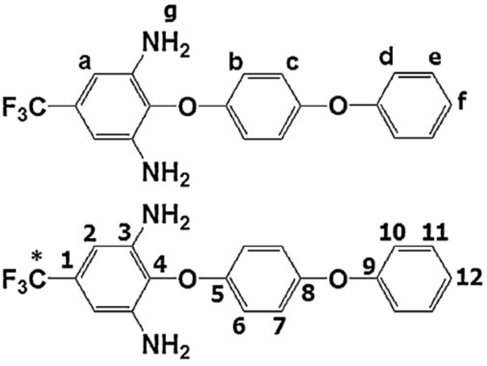

4.5. Synthesis of 2,6-bis(N-trimellitimido)-4-trifluoromethyl-4′-phenoxydiphenyl ether (TFPDPE)

AFPDPE (3.6033 g, 10 mmol), trimellitic anhydride (4.8025 g, 25 mmol), and glacial acetic acid (50 mL) were poured into a reaction flask. The heterogeneous mixture obtained was then refluxed under N_2 atmosphere for 15 h. Next, the reaction mixture was filtered to give a yellow precipitate. The precipitate was washed several times with hot ethanol to remove acetic acid residue. The product obtained was purified by recrystallization from DMF/H_2O. The solid obtained (TFPDPE) was then dried under reduced pressure at 100 °C for 24 h to afford 6.7313 g of yellow fine crystals (95% yield, m.p. = 365–368 °C). Results of the IR, ^{1}H NMR and ^{13}C NMR spectroscopy measurements of monomer TFPDPE are detailed below in Section 3.

4.6. Synthesis of poly(amide-imide)s

A typical example of TPP-activated polycondensation is described as follows. A mixture of TFPDPE (0.7086 g, 1 mmol), 2,6-diamino-4-trifluoromethyl-4′-phenoxydiphenyl ether (AFPDPE) (0.3603 g, 1 mmol), $CaCl_2$ (0.2 g), pyridine (1.2 mL), TPP (0.6 mL) and NMP (5 mL) were heated while being stirred at 100 °C for 3 h. The viscosity of the reaction solutions increased after 1 h, and an additional 3.0 mL of NMP were added to the reaction mixture. At the end of the reaction, the obtained polymer solution was trickled into stirred methanol. The yellow-stringy polymer was washed thoroughly with hot water and methanol, collected by filtration, and dried at 100 °C under reduced pressure. The calculated yield was about 95%. The limited viscosity number of the polymer obtained (TFPDPE/AFPDPE) was 0.62 dL/g. The other poly(amide-imide)s were synthesized in a similar manner.

Acknowledgments

Financial support from the Research Council of Islamic Azad University-Damghan branch (Ref No. 4409 projection/2 Tyr 1389) is greatly acknowledged. The authors are also grateful to the Sharif University of Technology for running the NMR spectra, Amir-Kabir University of Technology for running the TGA and DSC analyses, and University of Tehran for the SEM images.

References

[1] B. Sillion, R. Mercier, D. Picq, in: M.E. Rogers, T.E. Long (Eds.), Synthetic Methods in Step-Growth Polymers, Wiley, 2003, pp. 265–326.
[2] Q.J. Dautel, G. Wantz, D. Flot, J.P. Lere-Porte, J.J.E. Moreau, J.P. Parneix, F. Serein-Spirau, L. Vignau, J. Mater. Chem. 15 (2005) 4446–4452.
[3] J. Myung-Sup, L. Tae-Woo, H. Jingyu, H.S. Byung, J. In-Sun, Polymer 47 (2006) 2670–2676.

[4] M. Rubal, C.W. Wilkins, P.E. Cassidy, C. Lansford, Y. Yamada, Polym. Adv. Technol. 19 (2008) 1033–1039.

[5] B. Zhang, W. Li, J. Yang, Y. Fu, Z. Xie, S. Zhang, L. Wang, J. Phys. Chem. C 113 (2009) 7898–7903.

[6] G. Maier, Prog. Polym. Sci. 26 (2001) 3–65.

[7] C.L. Chung, W.F. Lee, C.H. Lin, S.H. Hsiao, J. Polym. Sci. Part A: Polym. Chem. 47 (2009) 1756–1770.

[8] J. Jin, D.W. Smith, C.M. Topping, S. Suresh, S. Chen, S.H. Foulger, N. Rice, J. Nebo, B.H. Mojazza, Macromolecules 36 (2003) 9000–9004.

[9] Y. Zhao, F. Wang, A. Li, B. Liu, Z. Wu, D. Zhang, S. Liu, M. Yi, Mater. Lett. 58 (2004) 2365–2368.

[10] G. Jiang, B. Yao, Y. Geng, Y. Chen, Z. Xie, L. Wang, X. Jin, F. Wang, Macromolecules 39 (2006) 1403–1409.

[11] T. Ma, S. Zhang, Y. Li, F. Yang, C. Gong, J. Zhao, J. Fluorine Chem. 131 (2010) 724–730.

[12] I.K. Shundrina, T.A. Vaganova, S.Z. Kusov, V.L. Rodionov, E.V. Karpova, E.V. Malykhin, J. Fluorine Chem. 132 (2011) 207–215.

[13] Y. Zhu, P. Zhao, X. Cai, W.D. Meng, F.L. Qing, Polymer 48 (2007) 3116–3124.

[14] S. Maji, S. Banerjee, J. Appl. Polym. Sci. 108 (2008) 1356–1364.

[15] X. Han, Y. Tian, L. Wang, C. Xiao, B. Liu, Eur. Polym. J. 43 (2007) 4382–4388.

[16] X.L. Wang, Y.F. Li, C.L. Gong, T. Ma, F.C. Yang, J. Fluorine Chem. 129 (2008) 56–63.

[17] A. Ghosh, S. Banerjee, High Perform. Polym. 21 (2009) 173–186.

[18] Y. Liu, Y. Zhang, S. Guan, L. Li, Z. Jiang, Polymer 49 (2008) 5439–5445.

[19] C.P. Yang, R.S. Chen, K.H. Chen, Colloid Polym. Sci. 281 (2003) 505–515.

[20] H. Choi, I.S. Chung, K. Hong, C.E. Park, S.Y. Kim, Polymer 49 (2008) 2644–2649.

[21] S. Banerjee, M.K. Madhra, A.K. Salunke, G. Maier, J. Polym. Sci. Part A: Polym. Chem. 40 (2002) 1016–1027.

[22] W. Jang, D. Shin, S. Choi, S. Park, H. Han, Polymer 48 (2007) 2130–2143.

[23] D.J. Liaw, K.L. Wang, F.C. Chang, Macromolecules 40 (2007) 3568–3574.

[24] Q. Mi, Y. Ma, L. Gao, M. Ding, J. Polym. Sci. Part A: Polym. Chem. 37 (1999) 4536–4540.

[25] H. Behniafar, H. Sadeghi-abendansari, Polym. Int. 61 (2012) 286–293.

[26] H. Behniafar, S. Mohammadparast-delshaad, Polym. Degrad. Stabil. 97 (2012) 228–233.

[27] H. Behniafar, N. Sefid-girandehi, M. Hosseinpour, J. Appl. Polym. Sci. (2012) (early view).

[28] H. Behniafar, M. Sedaghatdoost, J. Fluorine Chem. 132 (2011) 276–284.

[29] H. Behniafar, N. Sefid-girandehi, J. Fluorine Chem. 132 (2011) 878–884.

[30] H. Behniafar, A. Abedini-pozveh, Polym. Degrad. Stabil. 96 (2011) 1327–1332.

[31] N. Yamazaki, F. Higashi, Tetrahedron 30 (1974) 1323–1326.

[32] A. Banihashemi, H. Behniafar, Polym. Int. 52 (2003) 1136–1144.

[33] D. Braun, H. Cherdron, M. Rehahn, H. Ritter, B. Voit, Polymer Synthesis: Theory and Practice, Springer, 2005, pp. 104–112.